Photoregeneration of Bovine Rhodopsin from Its Signaling State†

Sophia Arnis and Klaus Peter Hofmann*

Institut für Medizinische Physik und Biophysik, Charité, Medizinische Fakultät der Humboldt-Universität zu Berlin, Ziegelstrasse 5-9, 10098 Berlin, Germany

Received March 24, 1995; Revised Manuscript Received May 12, 1995⊗

ABSTRACT: In rhodopsin, 11-*cis*-retinal is bound by a protonated Schiff base and acts as a strong antagonist, which holds the receptor in its inactive ground state conformation. Light induces *cis*-/*trans*-retinal isomerization and a sequence of thermal transitions through intermediates. The active conformation that catalyzes GDP/GTP exchange in the G-protein (G_t) is generated from the metarhodopsin II intermediate (MII) and mediated by Schiff base proton translocation and proton uptake from the aqueous phase. In the stable nucleotide-free MII−G_t complex, any thermal transition of MII into other forms of rhodopsin is blocked. We have now studied how G_t affects flash-induced photochemical conversions of MII. Difference spectra from measured absorption changes show that MII photolyzes through two parallel pathways, with fast (1 ms) and slow (50 ms) kinetics (12 °C, pH 6). The slow pathway regenerates rhodopsin (9- or 11-*cis*) via Schiff base reprotonation and proton release. We infer a *cis*-isomerized early photoproduct (reverted meta, RM) preceding these thermal transitions. When MII is photolyzed in the MII−G_t complex, the slow absorption change is abolished, indicating that G_t blocks the completion of the regeneration process. This is due to the formation of a stable RM−G_t complex, as shown by successive photolysis of MII, RM, and ground state rhodopsin, and the application of GTPγS at different stages. The complex dissociates with GTPγS, and rhodopsin relaxes to the ground state. The results indicate that *cis*-retinal and G_t can bind to the receptor at the same time. We discuss the result that the protonations in the meta II state uncouple retinal geometry from G_t interaction.

In rhodopsin's inactive ground state, 11-*cis*-retinal is bound by a protonated Schiff base (SB)[1] to residue Lys-296, located in the center of the last of the seven transmembrane stretches of the receptor; interaction with the SB counterion (Glu-113) and other noncovalent interactions within the membrane-embedded core of the protein tune the absorption to λ_{max} = 500 nm [for reviews, see Oprian et al. (1992), Fahmy et al. (1993), and Hargrave et al. (1993)]. After light-induced isomerization of the chromophore, the active meta II (MII, λ_{max} = 380 nm) state is generated after a sequence of spectrally defined intermediates [reviewed by Hofmann (1986), Nathans (1992), Lewis and Kliger (1992), Arnis and Hofmann (1993), and Fahmy and Sakmar (1992)]. MII formation depends on the neutralization of residue Glu-113, located on the third helix, by internal proton translocation from the still intact *trans*-retinal SB (Fahmy et al., 1993). Spectrally silent proton uptake from the aqueous phase occurs in a separate, later transformation of the protein; the meta II state thus has been further characterized as MII_a and MII_b, before and after proton uptake, respectively. Only in MII_b can rhodopsin form the cytoplasmic interaction domain for the G-protein, which involves residues on at least three of the four cytoplasmic loops (König et al., 1989; Hofmann & Kahlert, 1992). Proton uptake and formation of the signaling state depend on the ionization of the side chain of the highly conserved residue Glu-134, located near the cytoplasmic border of the third helix (Arnis et al., 1994; Fahmy & Sakmar, 1993). When rhodopsin (R) is solubilized in detergents such as dodecyl maltoside, the yield of MII_a from its meta I precursor is virtually complete. At sufficiently low pH, MII_b is stabilized with respect to MII_a and a quasi-irreversible reaction scheme applies (Arnis & Hofmann, 1993):

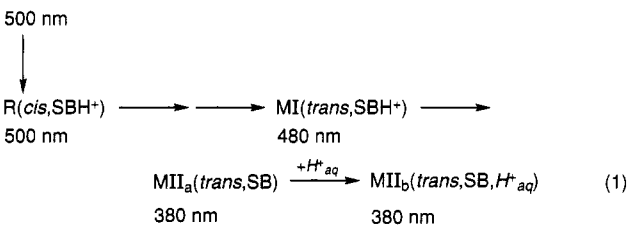

(1)

In this scheme, the intermediates are characterized by their chromophore conformation (*cis* or *trans*), their SB protonation (SBH^+) or deprotonation (SB), and the protonation state of the putative cytoplasmic G_t interaction surface (H^+_{aq}). The numbers given in nanometers indicate the wavelengths of irradiation (with downward arrow) and of maximal absorption of the intermediates formed. In the absence of guanine nucleotide, a stable complex is formed:

$$MII_B + G_t \longrightarrow MII_B - G_t \quad (2)$$

When GTP (or GTPγS) is added, the complex dissociates [see Hargrave et al. (1993)].

This work is an attempt to study the functional coupling between the G_t interaction domain and the retinal−pro-

† This work was supported by the Deutsche Forschungsgemeinschaft (SFB 60) and the Human Frontier Science Program.

⊗ Abstract published in *Advance ACS Abstracts,* July 1, 1995.

[1] Abbreviations: R, rhodopsin; MII, metarhodopsin II; MI, metarhodopsin I; MII_a, deprotonated form of MII; MII_b, protonated form of MII; P1 and P2, photolysis products of MII; RM and RR, intermediates of rhodopsin photoregeneration; BCP, bromocresol purple; DM, dodecyl maltoside; SB, (retinal) Schiff base; λ_{max}, wavelength of maximal absorption.

0006-2960/95/0434-9333$09.00/0

tein interaction domain in rhodopsin. We know that the interaction with G_t stabilizes the deprotonated SB configuration in MII_b and does not allow thermal transitions into SB protonated forms [MI or MIII; see Hofmann (1986) and Lewis and Kliger (1992)]. It therefore was of interest to investigate the photochemically induced reactions of the receptor in its G-protein-bound form.

MATERIALS AND METHODS

Rhodopsin Purification. Rhodopsin was purified in dodecyl maltoside (Boehringer, Mannheim, Germany) from disk membranes isolated from bovine rod outer segments as described; the experiments were carried out in a two-wavelength spectrophotometer developed by Hofmann and Emeis [see Arnis and Hofmann (1993)].

Flash Photolysis. Common to all experiments was an initial quantitative photoconversion of rhodopsin into MII by continuous illumination with $\lambda > 450$ nm for 20 s (optical system with a 100 W halogenium bulb, concave mirror, and condenser lenses; cutoff filter 450 nm). MII was then immediately photolyzed by 412 nm test flashes (20 μs, mole fraction of MII photolysis per flash was 0.8%, band-pass filter 412 $\pm$ 7 nm; at this wavelength, photoreversal of MII in the apparatus is optimized). Flash-induced differences in absorption (signals) were measured at two wavelengths simultaneously, with a 7 mm effective path length cuvette. The use of rhodopsin in dodecyl maltoside for these experiments, rather than in its native membrane environment, was motivated by the following reasons: (1) Photoconversion to MII (MII_a or MII_b, 380 nm) is virtually complete when rhodopsin is solubilized in octyl glucoside or dodecyl maltoside; in membranes however, the pH and temperature equilibrium between MI (478 nm) and MII (380 nm) allows such measurements only at low pH's and high temperatures. (2) In the dodecyl maltoside solution, and with an excess of G_t, all of the MII formed can bind to G_t. This is impossible in disk membranes because of the high density of rhodopsin, which limits the capacity to bind G_t.

Each experiment was reproduced at least three times with samples from different preparations.

RESULTS

Kinetic and Spectral Distinction of Two Parallel Pathways. Each measurement begins with quantitative conversion of the rhodopsin in the sample to MII (MII_a or MII_b, depending on pH; eq 1) by illumination for 20 s with wavelengths $\lambda >$ 450 nm. Subsequent immediate flash photolysis of MII with 412 nm test flashes yields photoproducts identified by their differences in absorption relative to MII. For the measurement of wavelengths throughout the visual range, the flash photometric absorption changes consist of a steplike (not time resolved) component and an additional component with a mean time around 50 ms (at 12 °C, pH 6). Difference spectra for the fast and slow components were obtained by fitting a sum of two exponentials to the signals (Figure 1). The spectra indicate that (i) the fast and the slow kinetic components belong to (at least) two different final products of MII photolysis with λ_{max} in the range of 470 or 500 nm, respectively, and that (ii) both of these photoproducts arise from near-UV precursors, because both difference spectra are negative in this range.

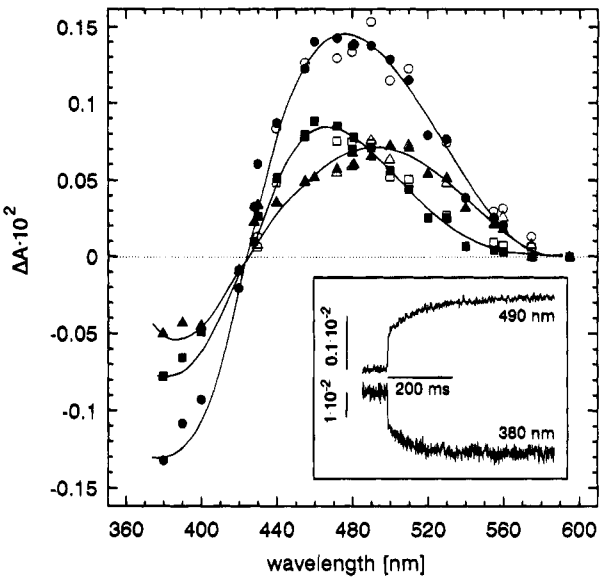

FIGURE 1: Difference spectra of absorption changes during meta-rhodopsin II (MII) photolysis. Spectra are shown for pH 6 (closed symbols) and pH 8 (open symbols). Rectangles and triangles are the amplitudes of the fast and slow components, respectively, and the total absorption change (circles) from 1 flash (for measuring wavelengths $\lambda > 430$ nm) or 30 flashes (for wavelengths $\lambda < 430$ nm, recorded over 30 s), with the amplitude of the absorption change extrapolated to flash 1. The solid lines are polynomial fits. Inset: Typical flash-induced absorption changes (signals) recorded at 490 (1 flash) and 380 nm (sum of 30 flashes), pH 6; vertical bars indicate the absorption change. Samples contained 5.8 μM rhodopsin, 130 mM NaCl, 50 mM MES (pH 6) or 50 mM BTP (pH 8), and 0.4 mM dodecyl maltoside; T = 12 °C.

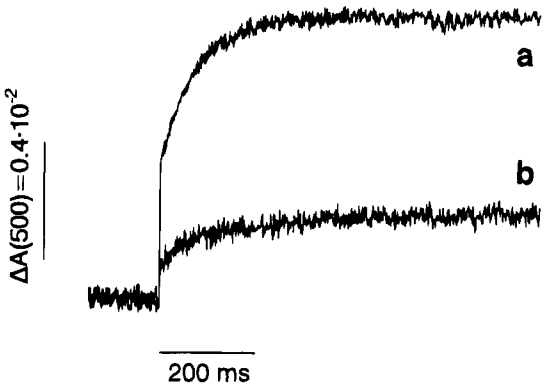

FIGURE 2: Flash-induced absorption changes of MII photolysis: (a) from a fresh sample; (b) after 100 min decay of MII. Signals are the absorption changes from 15 flashes (412 nm) measured at 500 nm, pH 6, and T = 18 °C. Sample the same as described for Figure 1.

Rhodopsin can be quantitatively photolyzed back and forth between the ground state and MII by alternating blue and yellow illumination. Absorption spectra taken after each illumination show that products with $\lambda_{max} \approx 380$ nm and $\lambda_{max} \approx 470-500$ nm are alternately formed (data not shown). When the MII in the sample is allowed to decay for 100 min before the remaining MII is photolyzed, the absorption change decreases but the relative weight of the fast and slow components remains the same (Figure 2). This shows that the decay products of MII do not contribute to the absorption change and that the decay does not select MII molecules reacting through the fast or slow pathway. Also, the relative weight of the components does not depend on pH (see the

following). Thus, the pool appears to be remain quite homogeneous, with no tendency to react through the fast or slow pathway preferentially. We can therefore state a reaction scheme,

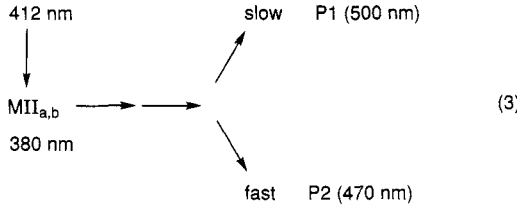

(3)

in which P1 and P2 are the final products of the slow and fast pathways, respectively (Figure 1). Double arrows indicate that several intermediates may occur (as shown for P1 in the following).

The data do not exclude P1 precursors, which may be buried in the fast absorption change; there is indeed a small shoulder in the P2 difference spectrum that may indicate such a product (Figure 1). Experiments with improved time resolution must be designed to obtain clear difference spectra and isosbestic points and to resolve the intermediates of the fast reaction sequence leading to the 470 nm product(s). However, we can state that, by their absorptions, both products P1 and P2 are protonated SB forms (Hofmann, 1986; Nathans, 1992; Oprian, 1993). Studies on rhodopsin (Williams, 1968) and bacteriorhodopsin (Druckmann et al., 1992) have suggested that the photolysis of SB-deprotonated MII or M states begins with light-induced isomerization of the chromophore and is completed by dark reactions, which lead to the final SB-reprotonated and conformationally changed state. During the dark reaction sequence, the chromophore conformation remains the one that was formed by the initial photochemical reaction. In our case, the position of the absorption maximum of the final product P1 is at 500 nm, reflecting the opsin shift to 500 nm typical for rhodopsin's ground state. This suggests that we may assume that the slow pathway is initiated by *all-trans*/11-*cis* isomerization; it may also contain a fraction of the functionally equivalent 9-*cis*-isorhodopsin (Williams, 1968; Okada et al., 1991). The chromophore conformation of the 470 nm product (P2) is unknown; by its absorption, it may be identified with 7-*cis* isoforms (Shichida et al., 1991). In the following sections, we will focus on the slow reaction pathway, which photoregenerates rhodopsin. It is of special interest because it depends on G_t.

trans-/cis-Retinal Isomerization and Schiff Base Reprotonation. According to the preceding discussion, we assume that photoreversal of MII begins with a photochemical step, yielding an intermediate in which the retinal is isomerized to *cis*, with the SB bond to Lys-296 still deprotonated. We will term this intermediate RM (reverted meta). It is important to note that the MII→RM reaction cannot be observed spectrophotometrically since RM is close in absorbance to MII (380 nm), and any small fast absorption change would be buried in the P2 jump (eq 3). The observable step is the reprotonation of the SB, which expresses itself in the large spectral shift to 500 nm (Figure 1). This yields a reaction scheme for the photoregeneration of rhodopsin in the P1 pathway:

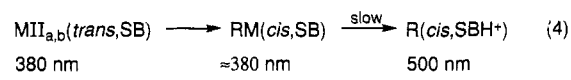

(4)

Schiff Base Reprotonation Depends on pH. Although the extent of photoregeneration is pH independent (Figure 1), its kinetics depends on pH. At pH 8, the slow component of the absorption change, indicating SB reprotonation, proceeds with faster kinetics than at pH 6 (Figure 3). For T = 8.5 °C, evaluation of the data yields $\tau_{1/2}$ = 45 ms at pH 8.0 and 100 ms at pH 6.0. This result is easily understood by the fact that SB protonation changes, occurring in milliseconds with high activatioin energy, reflect not only the proton translocation itself but also the accompanying transformation of protein structure (Arnis & Hofmann, 1993). Thus, Figure 3 reflects the difference in the thermal barrier between the reversal reaction to rhodopsin from MII$_b$ as compared to MII$_a$. This result is consistent with our previous interpretation of kinetic data on the R→MII forward reaction, which leads to the MII$_a$/MII$_b$ scheme (eq 1). It predicts that MII$_a$ is conformationally closer to the ground state than MII$_b$, so that photoregeneration can occur with faster kinetics. Arrhenius plots (Figure 3, inset) yield approximate activation energies E_a = 90 and 100 kJ/mol at pH 6 and 8, respectively.

Photoregeneration Is Completed by Proton Release. The work on the R→MII forward reaction has also shown that proton uptake from the aqueous milieu can only occur after SB deprotonation (eq 1). In analogy, we have now investigated the change in the state of protonation for the reverse pathway: Figure 4 shows simultaneous measurement of the SB reprotonation signal at 490 nm (isosbestic point of the pH indicator, bromocresol purple, BCP) and the absorption change of the BCP measured at 595 nm (absorption maximum of BCP). The negative absorption change reflects an acidification of the aqueous milieu, i.e., proton release by photolysis of MII. Calibration of the proton release signal by addition of HCl yields a release of 0.5 H^+ per MII photolyzed at pH 7. This is comparable to the proton uptake per photolyzed rhodopsin at this pH (Arnis & Hofmann, 1993) and may be interpreted as the reversal of the forward reaction in eq 1.

Remarkably, proton release is 3 times slower ($\tau_{1/2}$ = 250 ms at pH 7 and 12 °C) than the SB reprotonation seen at 490 nm (Figure 3). This indicates a spectrally silent transformation of the protein, reflected in proton release, which occurs after SB reprotonation. An isochromic precursor of the fully relaxed state is thereby indicated in which the SB is reprotonated, but proton exchange with the aqueous phase has not yet occurred (photoproduct RR). The overall reaction may follow a sequence of retinal isomerization, SB proton translocation, and proton exchange with the aqueous phase, analogous to the forward reaction in eq 1:

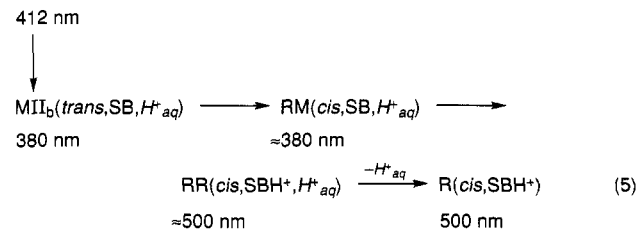

(5)

The data do not give an answer about the positions of thermodynamic equilibria in eq 5. It is important to note again that eq 5 describes the slow P1 pathway in eq 3. A

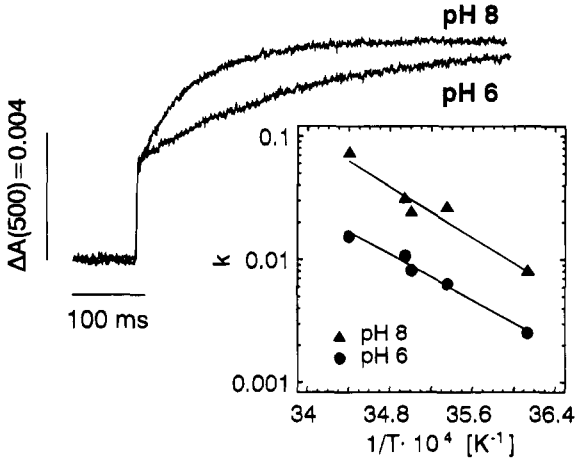

FIGURE 3: Flash photolysis of MII at pH 6 (MII_b) and pH 8 (MII_a). Signals are the absorption changes from 15 flashes (412 nm) measured at 500 nm. Samples contained 2 μM rhodopsin, 50 mM MES (pH 6) or 50 mM BTP (pH 8), 130 mM NaCl, and 0.4 mM dodecyl maltoside; T = 8.5 °C. Inset: Arrhenius plots of the slow component.

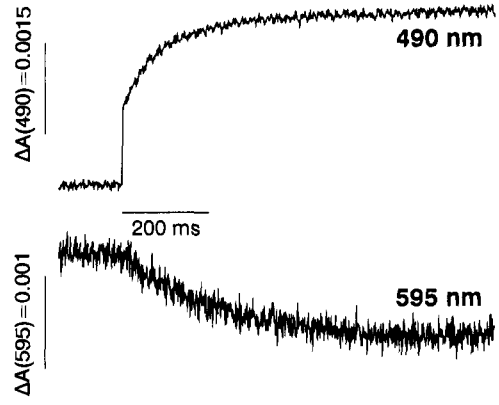

FIGURE 4: Schiff base reprotonation and proton release during MII photolysis. Protocol as described for Figure 1. MII photolysis and proton release were recorded simultaneously at 490 and 595 nm, respectively. Signals are the absorption changes from two flashes. MII photolysis was measured as in Figure 1, and proton release was determined by the absorption change of bromocresol purple indicator dye (λ = 595 nm, isosbestic point 490 nm). All samples contained 5.8 μM rhodopsin, 130 mM NaCl, 12.3 μM bromocresol purple, and 0.4 mM dodecyl maltoside, pH 7; T = 12 °C. Preparation of the buffer-free sample was as described (Arnis & Hofmann, 1993).

similar scheme may apply to P2, as similar steps are also found for the fast photoregeneration in the case of bacteriorhodopsin (Druckmann et al., 1992).

Effect of the G-Protein on Photoregeneration. In the presence of excess G_t (2 μM G_t, 1 μM rhodopsin) and the absence of nucleotide, the MII formed by a green flash from rhodopsin is quantitatively (>95%; Kahlert et al., 1990) bound to G_t. Low pH supports complex formation because it favors the active species MII_b over MII_a (eqs 1 and 2). When MII−G_t is photolyzed under these conditions (pH 6), the slow component of the MII photolysis signal (P1 in eq 3) is suppressed (Figure 5A, left). At pH 8, a small fraction of the MII is present as free MII_a in the coupled equilibrium of free and G_t-bound MII forms (reaction scheme: $MII_a \rightleftharpoons MII_b \rightleftharpoons MII_b{-}G_t$). In this case, the suppression is less pronounced, and a very slow (pseudo-zero-order) photoregeneration via the MII_a bottleneck is seen (Figure 5A, right). Figure 5B confirms that G_t suppresses only the slow

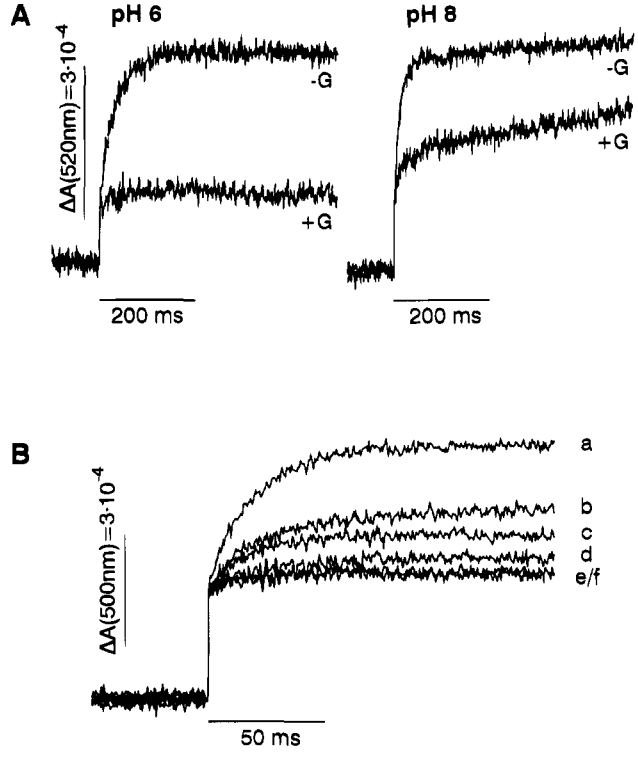

FIGURE 5: Photolysis of MII in the presence of G_t. (A) Flash photolysis. Effect of G_t on MII flash photolysis at pH 6 and 8; protocol as for Figure 1. Absorption changes from 15 flashes (412 nm), in the presence and absence of G_t, were recorded at 520 nm; the slow signal component dominates at this wavelength (Figure 1). Samples contained 1 μM rhodopsin, 2 μM G_t, 130 mM NaCl, and 0.4 mM dodecyl maltoside, pH 6; T = 18 °C. (B) Graded effect on MII flash photolysis by increasing amounts of G_t: 1 μM rhodopsin and 0 (a), 1.2 (b), 1.6 (c), 2.0 (d), 3.0 (e), and 4.0 (f) μM G_t, pH 6; T = 18 °C. It is seen that the G-protein only affects the slow component of the absorption change. Absorption changes from 20 flashes (412 nm), in the presence and absence of G_t, were recorded at 500 nm.

component of the absorption change. It is seen that the slow component decreases gradually with increasing G_t concentration and that even excess G_t does not affect the fast component. [The difference spectrum for the total absorption change with excess G_t is the same as the one with excess G_t (data not shown).]

The experiment shows that photolysis of MII in the complex with G_t does not photoregenerate rhodopsin's ground state. The fact that the fast component is not affected indicates that either the G-protein does not bind to P2 or the photolytic pathway does not depend on it (see the Discussion).

Three-Step Illumination Protocol. Since G_t blocks photoregeneration, the question that arises is which of the photolytic intermediates identified in eq 5 can exist in complex with G_t. Since no reprotonation signal (λ_{max} = 500 nm) is seen, RR is excluded. The crucial question is whether RM−G_t can be formed from MII_b−G_t, i.e., whether the *cis* conformation of the chromophore is tolerated by bound G_t. RM cannot be distinguished from MII by its absorption, but a functional test can give an answer. It is based on the ability of free RM to regenerate the ground state in the dark; we also use the properties that the products of MII photolysis in pathways P1 and P2 are reconvertible to MII with yellow light and that GTP and its analog GTPγS dissociate G_t from its complex with active forms of the receptor.

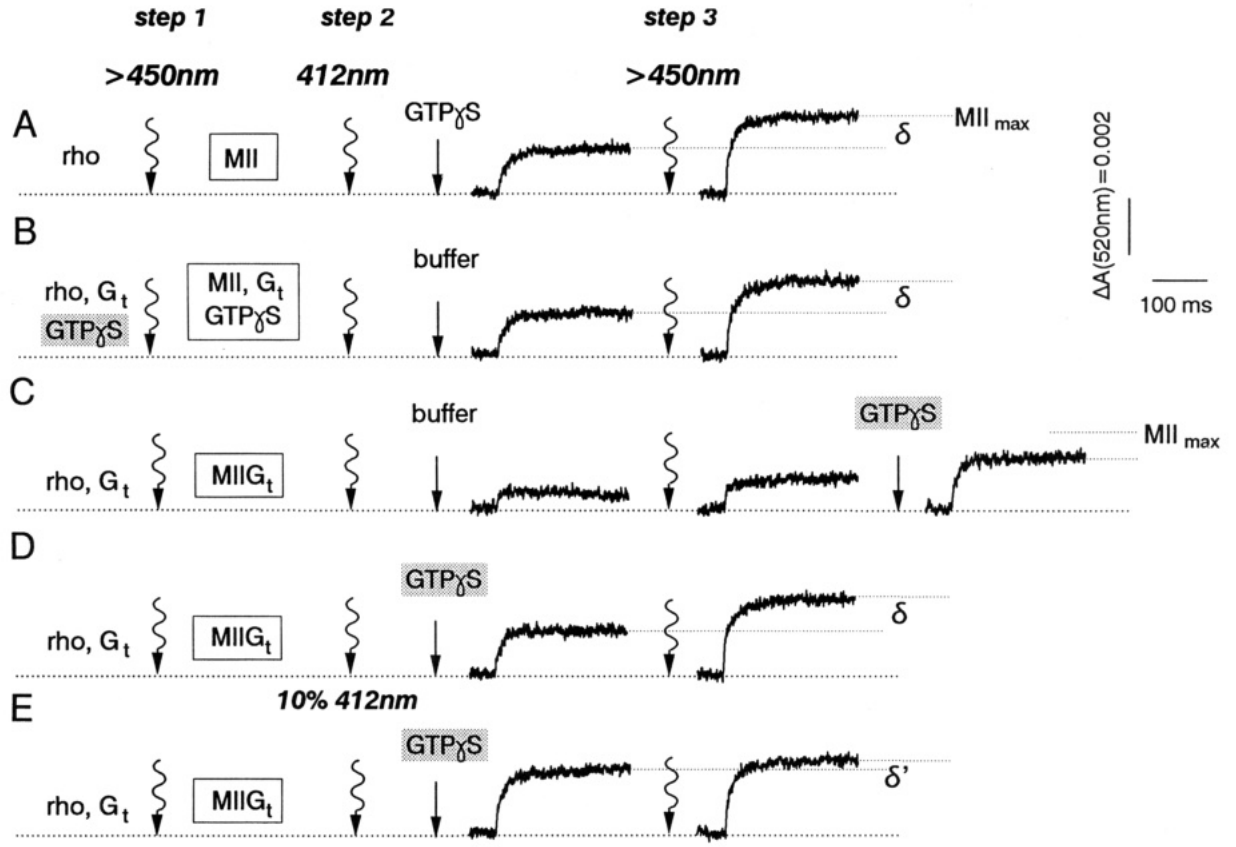

FIGURE 6: Effect of nucleotide on the MII_b-G_t complex and its photolysis products. (A) Three-step experimental scheme: step 1, photoconversion of rhodopsin into MII_b by illumination with $\lambda > 450$ nm; step 2, photolysis of 40% of free MII_b (no G_t present; illumination by 100 flashes, $\lambda = 412$ nm; photolysis per flash 0.8%; test signal 15 flashes, 412 nm); step 3, quantitative photoconversion (20 s of continous illumination, $\lambda > 450$ nm) of the photolysis products arising from step 2 (test signal as in step 2). Repetition of protocol A starting from (B) rhodopsin, G_t, and GTPγS; (C) rhodopsin and G_t with addition of GTPγS after step 3; (D) rhodopsin and G_t with addition of GTPγS after step 2; (E) repetition of (D) with weaker (10%) 412 nm illumination in step 2. Samples contained 1.4 μM rhodopsin, 130 mM NaCl, 50 mM MES, and 0.4 mM dodecyl maltoside; GTPγS added was 180 μM, pH 6, T=18 °C. δ (δ') is the difference in amplitude between the test signals after steps 2 and 3 (for details see text). We note that the decay of MII forms to metarhodopsin III is negligible under the conditions of the experiment (data not shown).

The three-step protocol is as follows: (1) As in the experiments described earlier, rhodopsin is (in the absence or presence of G_t) quantitatively transformed into MII (MII_b, pH 6) or $MII-G_t$ (illumination for 20 s with $\lambda > 450$ nm). (2) Subsequently, approximately 40% of the MII (respectively $MII-G_t$) formed in step 1 is photolyzed by illumination with $\lambda = 412$ nm (100 flashes, same as used for the test flashes in the experiments earlier (Figures 1−5). (3) Yellow illumination (same as in step 1) causes the back-isomerization of all products that absorb at wavelengths >450 nm, i.e., of the protonated Schiff bases in pathways P1 and P2 (eq 3). After steps 2 and 3, test signals (each the average of 15 test flashes, 412 nm, monitoring wavelength was 520 nm) probe the amount of free MII (only from free, uncomplexed MII is rhodopsin photoregenerated; Figure 5). The turnover by the 15 test flashes is not negligible compared to the conditioning 412 nm illumination (100 flashes) in step 2, but the error is small enough to allow the necessary conclusions. Addition of GTPγS after steps 2 or 3 probes the effect of the nucleotide on the photoproducts present.

Effect of GTPγS. The first line (A) in Figure 6 explains the illumination scheme. Illumination with $\lambda > 450$ nm (step 1) converts rhodopsin into MII, and the subsequent 412 nm illumination (step 2) reconverts part of the MII (40%) back to rhodopsin (P1) and the P2 product(s). The first test signal reflects the relative amount of MII (60%) that remained after this conversion. In step 3, the sample is subsequently illuminated with $\lambda > 450$ nm, which converts the products arising from 412 nm photolysis back to MII. The second test flash again probes the pool of MII. The difference δ between the test signals reflects the amount of MII sequestered in form P1 or P2 after step 2, which become visible (i.e., sensitive to the 412 nm test flash) only after reconversion to MII with yellow light (in step 3). Since no G_t is present, all of the RM is free to decay to R and is then fully reconverted to MII_b; thus, MII_{max} reflects the maximal amount of MII_b that can be recruited in the cyclic protocol. GTPγS had no influence on rhodopsin or its photoproducts; it was added only to keep the conditions identical for all measurements.

When the protocol is repeated in the presence of G_t and GTPγS (Figure 6B), the test flashes evoke signals identical to the ones without any G-protein (Figure 6A); this is expected because the $MII-G_t$ complex dissociates with GTPγS [see Hofmann and Kahlert (1992)], and only free MII is present from the very beginning.

When GTPγS is added after the 412 nm illumination (Figure 6C−E), the nucleotide acts on MII (60% of the total opsin present) and on the MII photolysis products. In Figure 6C, GTPγS was added only after step 3. Small test signals are measured after steps 2 and 3, reflecting the lack of free MII, which is bound in stable complexes. The first test signal (after step 2) is from the MII that goes through the fast, G_t independent (Figure 5) P2 pathway; its amplitude, relative

to the ones in lines A or B, should be ca. 1/3 (ratio of fast component to total absorption change at 520 nm; cf. Figure 1). The measured value (0.4) is consistent with the notion that MII remains tightly bound to G_t and does not spontaneously dissociate in the absence of GTP. The amplitude after the subsequent 450 nm illumination (step 3) is somewhat larger, indicating that the P2 products formed in step 2 (and by the test flashes) were reconverted to MII.

The test signal after subsequent addition of GTPγS is much larger, but it does not reach the maximal amplitude. Both observations are important. The signal corresponds to the amount of MII that is released by GTPγS from its complex with G_t and sensitive to the test flash. The difference from MII_{max} must be due to products that remained sequestered and were not sensitive to step 3 illumination because of their near-UV absorption. RM$-G_t$ was identified earlier as the product with these properties. It is sensitive to GTPγS, as will be shown in the following, but it has reacted with rhodopsin and therefore does not contribute to the test signal. Overall, the experiment in Figure 6C excludes spontaneous dissociation of the MII$-G_t$ and/or RM$-G_t$ complexes under the conditions and the time frame of the three-step experiment.

When GTPγS is added immediately after step 2 (Figure 6D), the first test signal reflects the fraction of MII that was not photolyzed (60%) and comes from the dissociation of the MII$-G_t$ complex by GTPγS. It is identical to the controls (A, B), and it is smaller than MII_{max} by the same difference δ. Repetition of the protocol with weaker 412 nm illumination (10% neutral glass filter; Figure 6E) yields a much smaller difference δ'. According to the reaction scheme (eq 5), the difference is due to RM that was formed by the 412 nm illumination in step 2 and remained in complex with MII. This assignment is confirmed by the third test signal, which reaches the full amplitude MII_{max}. An explanation consistent with all results is that the RM$-G_t$ complex was dissociated by GTPγS and the released RM reacted in the dark with rhodopsin, which by the subsequent illumination in step 3 (λ > 450 nm) became reconverted to MII and sensitive to the test flashes.

RM Forms a GTP-Sensitive Complex with G_t. These data demonstrate that (i) 412 nm photolysis products must exist that are arrested by bound G_t in a form different from MII (otherwise MII_{max} would be seen with the first test flash) and (ii) GTPγS can dissociate the G_t-bound products and make them available for reconversion to MII with λ > 450 nm. With eq 3 RM is identified as the species that forms a stable complex with G_t and blocks photoregeneration. The experiments do not answer the question whether products of the P2 pathway can form a complex with G_t.

DISCUSSION

Normal and Reverse Photolysis of Rhodopsin. This study started from the notion that rhodopsin exists in two significant states, namely, the light sensitive ground state and the active meta II state, in which the receptor interacts with the G-protein G_t. From physiological and mechanistic perspectives, both the avid catalytic activity of the meta II and the virtually absolute inactivity of the ground state are of interest. In the ground state, rhodopsin bears 11-*cis*-retinal in its hydrophobic core; the covalent link to Lys-296 via a protonated retinal Schiff base (SB), its stabilization by the counterion Glu-113, and other interactions with the apoprotein hermetically lock the receptor against any interaction with other proteins. The receptor inevitably needs to absorb a light quantum to leave this state. As far as we know, the trigger event for any transformation of the protein is isomerization of the retinal from a *cis* into a *transoid* geometry. The subsequent transformations in the dark include translocation of the SB proton to its counterion at Glu-113 (Fahmy et al., 1993) and proton uptake from the aqueous phase involving Glu-134 (Arnis et al., 1994) to generate the meta II state.

There is no light independent reaction pathway that leads from meta II directly back to the ground state. Meta II needs to go through its decay (Hofmann, 1992) and be regenerated with 11-*cis*-retinal provided by the metabolism of the retina. However, the ground state can be regenerated by light directly from the deprotonated SB, albeit with small quantum efficiency (Williams, 1968). In this study, we could directly demonstrate two of the necessary steps for photoregeneration, namely, Schiff base reprotonation and proton release. For the photochemical trigger step, which must precede any thermal transition, we have assumed a reverse *trans/cis* isomerization of the retinal. Direct proof of this assumption as it exists for the forward reaction is lacking. However, the isomerization mechanism is consistent with the available data (Williams, 1968; Druckmann et al., 1992; this work), and it is, at the present state of our knowledge, the only explanation for the initial uptake of photochemical energy into a retinal protein. By introducing the intermediates RM, RR, and R, one obtains the reaction schemes for the forward (eqs 1 and 6) and reverse (eq 7) reactions:

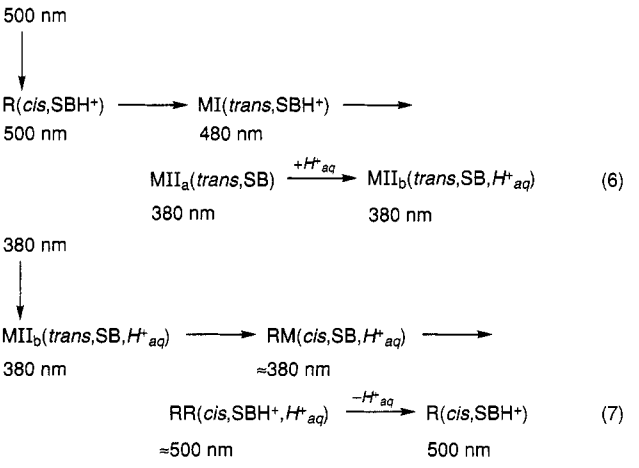

The reaction pathways display a fundamental similarity. Photoreversal does not reverse the forward sequence of events, but again, the reaction sequence proceeds through isomerization, proton translocation, and change of protonation of the G_t-interacting surface (note that, in contrast to the equations earlier, the wavelength of the photolyzing light is now given as the one of maximal efficiency).

Equation 7 was not the only pathway of MII photolysis observed. There is a fraction of MII that cannot form the properly regenerated, light-activatable ground state. The parallel pathway (P2 in eq 3) is much faster and ends in a 470 nm form with unknown chromophore geometry and functional properties. Here, we must leave this form out of consideration.

Effect of the G-Protein. To test the effect of bound G_t, we made use of the fact that, even in detergent, G_t binds—in

the absence of nucleotide—very tightly to MII. Under conditions that favor the protonated form, MII_b, a near-UV flash applied to a sample that contains MII and an excess of G_t hits virtually no free MII but only MII_b—G_t complexes. Under such conditions, the last two steps in the reaction sequence (eq 7) are blocked, as seen in the absence of any SB reprotonation signal (Figure 5). An obvious explanation of this result would be that the apoprotein, locked in the G_t complex, would have no access to any other chromophore configuration but meta II. However, the experiments in Figure 6 show that the RM—G_t complex exists and that it is the form in which the regeneration pathway is arrested. The activating cofactor GTPγS dissociates the complexes, so that G_t (in its GTP-binding form) and free ground state rhodopsin (distinguished from RM and MII by its sensitivity to yellow light, Figure 6) can be formed.

Thus, an isomerized configuration of retinal can be formed while rhodopsin interacts with the G-protein. The complex with the G-protein remains GTP sensitive, as it is in MII. The relaxation in the dark to ground state rhodopsin strongly suggests that retinal adopts the 11-*cis* (or 9-*cis*) configuration while it interacts with the G-protein. 11-*cis*-Retinal is a prototype of a "negative antagonist", defined as a ligand that stabilizes the inactive conformation of a receptor (Lefkowitz, 1993). Determinants for the apoprotein to accommodate 11-*cis*-retinal and G_t at the same time include that the retinal Schiff base is deprotonated and the relevant sites in the G_t interaction domain are protonated. Recent studies have suggested that, in this state of protonation, the side chains of residues Glu-113 and Glu-134 are neutralized (Fahmy & Sakmar, 1993; Arnis et al., 1994). Both of these residues are located within the third helix of rhodopsin's seven-helix structure. The resulting charge distribution around the third helix appears to provide the interface between bound G_t and the antagonistic conformation of the chromophore. A logical extension of this work therefore is to investigate mutants in which this charge distribution is anticipated; they should display activity toward G_t, even when 11-*cis*-retinal is bound. Such investigations are underway (S. Arnis, K. P. Hofmann, and T. P. Sakmar, unpublished results).

Energetics. Binding of G_t in the nucleotide-free complex in this study served to stabilize the receptor interaction domain. The free energy of G_t binding is not known, but an upper limit is given by the GTP/GDP free energy gap, which must drive both the receptor/G-protein and G-protein/effector association/dissociation cycles. This means an energy is imposed on the receptor interaction domain on the order of 20—40 kJ/mol. Thus, we can conclude that the free energy of coupling between chromophore—protein and protein—protein interactions (domains A and B in Figure 7) must be lower than this intermolecular energy. Otherwise, we would not observe isomerization of the chromophore without release of the bound G_t. The subsequent blockade by G_t of the RM—RR transition shows that the binding energy of G_t can, in this state of protein relaxation, overcome the tendency of the protein to reprotonate the SB. In future work, it will be of interest to determine the energy uptake into the protein by isomerization of the SB deprotonated retinal in the meta II state. If it were 140 kJ/mol (as it is in the forward rhodopsin—batho conversion; Cooper, 1979), the fraction of photochemical energy flowing into coupling with the G_t binding sites could be only a few percent.

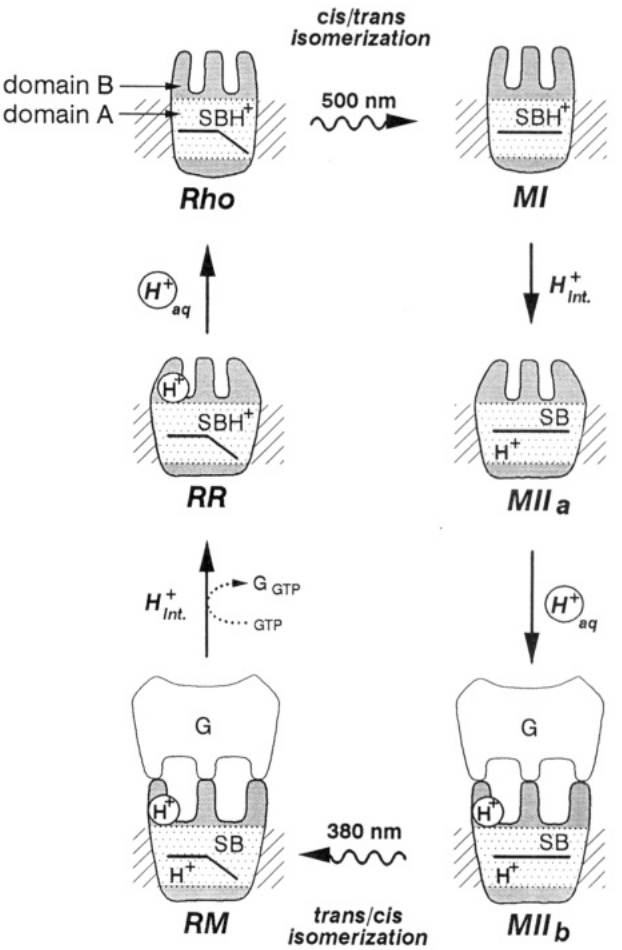

FIGURE 7: Reaction model of rhodopsin activation and photoregeneration. Activity of rhodopsin (Rho) depends on SB proton translocation (H^+_{int}) in domain A and proton uptake (H^+_{aq}) in domain B. Bent or straight bars indicate *cis*- or *trans*-retinal, respectively; hatched regions indicate the detergent. Shown here are the dark reactions of activation (right) and light-induced deactivation (photoregeneration, left) and the photochemical trigger reactions (*cis*/*trans*, top, or *trans*/*cis*, bottom). Activation or deactivation passes through one of the intermediate states, MII_a or RR. In states MII_b or RM (bottom), both domains, A and B, are active. All three states of the receptor, inactive (top), intermediate (middle), and active (bottom), can bear retinal in its *cis* (left) or *trans* (right) conformation. The photoregeneration of rhodopsin from MII_a via RM is omitted for clarity. See text for details.

Two Functional Domains in Rhodopsin. In a previous study (Arnis & Hofmann, 1993), the notion of two different forms of meta II, MII_a and MII_b, was based on the kinetics of light-induced meta II formation and proton uptake. Subsequent work has attributed proton uptake to the cytoplasmic interaction surface (Arnis et al., 1994). Different forms of meta II indicate then that an inactive or active cytoplasmic interaction domain can coexist with one and the same state of SB protonation. This has provided the first evidence for a certain conformational independence between these two domains of rhodopsin. The present study extends this concept. A comprehensive reaction model is shown in Figure 7. Rhodopsin comprises two functional domains, A and B. Necessary for activation is SB proton translocation (H^+_{int}) in domain A and proton uptake (H^+_{aq}) in domain B. Shown in the figure are the dark reactions of activation (Figure 7, right) and light-induced deactivation (photoregeneration, left) and the photochemical trigger reactions (*cis*/

trans, top, or *trans/cis*, bottom). The receptor exists in three different states: inactive (top), intermediate (middle), and active (bottom). Activation or deactivation passes through one of the intermediate states, MII_a or RR. The stabilizing interaction with the G-protein requires that both domains, A and B, be in their active state (bottom). All three states of the receptor, inactive, intermediate, and active, can exist with the retinal in its *cis* (left) or *trans* (right) conformation.

Evaluation of the SB reprotonation kinetics allows a statement about the cross-talk between the domains. It was found that, if photoregeneration starts from the protonated form of meta II, MII_b, the reaction is a factor of 3 slower than if photoregeneration starts from MII_a (Figure 4). This is consistent with the additional pH dependent barrier it has to overcome and shows that, during reformation of the protonated Schiff base, the protein is already sensitive to the pH dependent protonation of groups that exchange with the aqueous environment. Interestingly, the activation energy for SB reprotonation is smaller (100 kJ/mol) than that for its deprotonation in the forward reaction (MII formation, 160 kJ/mol; Arnis & Hofmann, 1993). This indicates that proton translocation is linked to different protein transformations in the forward vs backward reactions, presumably reflecting the influence of the different chromophore conformations in MII_a vs RR.

Potential Role of the New Product RM in the Visual Process. The finding of a *cis*-retinal−opsin−G_t complex may be relevant for the spontaneous dark activity of single rhodopsin molecules (Baylor et al., 1987; Leibrock et al., 1994). It was explained recently by successive Schiff base deprotonation and thermal *cis/trans* isomerization (Birge, 1993). Given the degree of independence between the domains of chromophore−protein and protein−G_t interactions in the meta II state, an interesting alternative may be envisaged. The G_t interaction domain may even form spontaneously and without the necessity of thermal isomerization of the chromophore.

ACKNOWLEDGMENT

We thank Oliver Ernst and Stefan Jäger for helpful discussions.

REFERENCES

Arnis, S., & Hofmann, K. P. (1993) *Proc. Natl. Acad. Sci. U.S.A. 90*, 7849−7853.
Arnis, S., Fahmy, K., Hofmann, K. P., & Sakmar, T. P. (1994) *J. Biol. Chem. 269*, 23879−23881.
Baylor, D. A., Matthews, G., & Yau, K.-W. (1987) *J. Physiol. 309*, 591−621.
Birge, R. R. (1993) *Biophys. J. 64*, 1371−1372.
Cooper, A. (1979) *Nature 282*, 531−533
Druckmann, S., Friedman, N., Lanyi, J. K., Needleman, R., Ottolenghi, M., & Sheves, M. (1992) *Photochem. Photobiol. 56*, 1041−1047.
Fahmy, K., & Sakmar, T. P. (1993) *Biochemistry 32*, 7229−7236.
Fahmy, K., Jäger, F., Beck, M., Zvyaga, T. A., Sakmar, T. P., & Siebert, F. (1993) *Proc. Natl. Acad. Sci. U.S.A. 90*, 10206−10210.
Franke, R. R., Sakmar, T. P., Graham, R. M., & Khorana, H. G. (1992) *J. Biol. Chem. 267*, 1467−1474.
Hargrave, P. A., Hamm, H. E., & Hofmann, K. P. (1993) *BioEssays 15*, 43−50.
Hofmann, K. P. (1986) *Photobiochem. Photobiophys. 13*, 309-338.
Hofmann, K. P., & Kahlert, M. (1992) in *Signal Transduction in Photoreceptor Cells* (Hargrave, P. H., Hofmann, K. P., & Kaupp, U. B., Eds.) pp 71−102, Springer-Verlag, Berlin.
König, B., Arendt, A., McDowell, J. H., Kahlert, M., Hargrave, P. A., & Hofmann, K. P. (1989) *Proc. Natl. Acad. Sci. U.S.A. 86*, 6878−6882.
Lefkowitz, R. J. (1993) *Nature 365*, 603−604.
Leibrock, C. S., Reuter, T., & Lamb, T. D. (1994) *Vision Res. 34*, 2787−2800.
Lewis, J. L., & Kliger, D. S. (1992) Photointermediates of visual pigments, *J. Bioenerg. Biomembr. 24*, 201−210.
Nathans, J. (1992) *Biochemistry 31*, 4924−4931.
Okada, T., Kandori, H., Shichida, Y., Yoshizawa, T., Denny, M., Zhang, B.-W., Asato, A. E., & Liu, R. S. H. (1991) *Biochemistry 30*, 4796−4802.
Oprian, D. D. (1992) *J. Bioenerg. Biomembr. 24*, 211−216.
Shichida, Y., Kandori, H., Okada, T., & Yoshizawa, T. (1991) *Biochemistry 30*, 5918−5926.
Williams, T. P. (1968) *Vision Res. 8*, 1457−1465.

BI9506684